Poly[(diphenylsilanediyl)ethynediyl]: Structure and Optical and Electroluminescent Properties

Stanislav Nešpůrek,[1,2] Petr Toman,[1] Akihiko Fujii,[3] Katsumi Yoshino[3]

[1]*Institute of Macromolecular Chemistry, Academy of Sciences of the Czech Republic, Heyrovský Square 2, 162 06 Prague 6, Czech Republic*
[2]*Faculty of Chemistry, Technical University of Brno, Purkyňova 118, 612 00 Brno, Czech Republic*
[3]*Department of Electronic Engineering, Faculty of Engineering, Osaka University, 2-1 Yamada-Oka, Suita, Osaka 565, Japan*

Received 11 March 2006; accepted 28 July 2006
DOI 10.1002/app.26084
Published online in Wiley InterScience (www.interscience.wiley.com).

ABSTRACT: Poly[(diphenylsilanediyl)ethynediyl] with a band-gap energy of 5.2 eV is a wide-band-gap material with a photoluminescence maximum at a wavelength of 354 nm. It is suitable for the fabrication of ultraviolet electroluminescence diodes. The electroluminescence spectrum consists of a strong peak at 361 nm and a tail up to 570 nm. The external quantum emission efficiency at the main maximum, calculated in terms of emitted photons per transported electronic charge, is 0.01% (no sample optimization has been carried out). The electric characteristics are controlled by contact-limited currents and double injection. The geometry of the neutral oligo[(diphenylsilanediyl)ethynediyl] molecule and its infrared spectra and the changes in the geometries and charge distributions during the formation of the positive and negative ions have been calculated by quantum chemical methods. © 2007 Wiley Periodicals, Inc. J Appl Polym Sci 105: 208–214, 2007

Key words: charge transport; light-emitting diodes (LED); quantum chemistry

INTRODUCTION

The first reports of electroluminescence (EL) in organic materials appeared for anthracene crystals in 1965.[1] A variety of studies[2] of the mechanisms of the transport, injection, and trapping of charge carriers ensued, but the difficulties associated with single-crystal growth and the high voltages required for macroscopic samples restricted practical applications. Later, Tang and coworkers[3,4] fabricated analogous devices based on thin ($\sim$ 100 nm) evaporated films of tris(quinolin-8-olato)aluminum, which operated at 10 V. Further attention was drawn by the advent of similar devices fabricated by Burroughes et al.[5] based on the conjugated polymer poly(1,4-phenylenevinylene) (PPV), which could be formed by a simple technology via spin casting from a solution and a subsequent thermal treatment. The development of solubilized conjugated polymers makes this a potentially attractive approach for the simple fabrication of light-emitting diodes (LEDs). At present, many conjugated polymers with π-electron systems in their main chains and polysilanes with one-dimensional, delocalized σ-electron systems along Si backbones are used for the preparation of LEDs and for studies of their properties.[6] π-Conjugated polymers, such as substituted PPV,[7] exhibit EL mainly in the visible region, which is interesting for potential applications in large-area, flat displays. σ-Conjugated polymers, which transport holes very well and emit mainly blue light, such as polysilanes,[8,9] are worth mentioning. The charge-carrier mobility of poly[methyl(phenyl)silylene] (PMPSi) was found to be approximately 10^{-8} m^2 V^{-1} s^{-1}.[10,11] Recently, PMPSi was used as a hole-transporting material in a multilayer EL device consisting of an indium tin oxide (ITO) electrode, PMPSi, 3-(benzothiazol-2-yl)-7-(diethylamino)coumarin-doped polystyrene, a vacuum-deposited layer of tris(quinolin-8-olato)aluminum as an electron-transporting material, and an Al electrode.[12] Even when the technologies of the fabrication of LEDs are developed at a very high level,[13] there is still strong interest in the preparation of devices emitting ultraviolet (UV) light.[14]

An attempt has been made to synthesize polymers whose backbone consists of both σ-conjugated Si structures and π-conjugated oligophenylene units.[15]

This article is dedicated to the memory of the Professor Marian Kryszewski.

Correspondence to: S. Nešpůrek (nespurek@imc.cas.cz).

Contract grant sponsor: Czech Science Foundation; contract grant number: 203/06/0285.
Contract grant sponsor: Grant Agency of the Academy of Sciences of the Czech Republic; contract grant number: 100100622.
Contract grant sponsor: Academy of Sciences of the Czech Republic (through the Information Society program); contract grant number: T400500402.

The optical absorption has been found to be influenced by both the oligosilane and oligophenylene parts, and the photoluminescence (PL) is shifted to the visible region in comparison with that of a σ-conjugated skeleton. PL is more influenced by the oligophenylene part of the main chain. The Stokes shift is slightly larger than that of the corresponding phenylene oligomers but much larger than that of the corresponding oligosilanes. The large Stokes shift (up to 1.3 eV) indicates that this type of substance is a good candidate for lasing. A remarkable spectral narrowing upon irradiation with 355-nm light from a Nd:YAG laser has been observed for poly[(tetraethyldisilane-1,2-diyl)-*p*-quaterphenyl-diyl]. In this article, we report on the spectral and EL properties of a polymer consisting of carbon and silicon atoms in the main chain with the carbon atoms bonded by a π-electron-containing triple bond: poly[(diphenylsilanediyl)ethynediyl] (PDPSiEt). The silicon atoms are substituted with π-conjugated phenyls.

EXPERIMENTAL

PDPSiEt (see Scheme 1) was prepared by the condensation of dichloro(diphenyl)silane with tetrachloroethane in a way similar to that described by Fang et al.[16] The low-molecular-weight fraction was extracted with boiling diethyl ether. The polymer possessed a unimodal but broad molar mass distribution [weight-average molecular weight = 4×10^3 g/mol, molar mass distribution (weight-average molecular weight/number-average molecular weight) = 2.72]. Before the deposition of the films, the polymer was three times reprecipitated and centrifuged (12,000 rpm, 15 min). After deposition, the films were dried at 10^{-3} Pa and at 330 K for at least 4 h.

Films for PL measurements were prepared from a toluene solution by spin coating (2000 rpm, 50 s) or by casting onto stainless steel substrates. The thickness of the films was around 500 nm. The EL diodes consisted of an ITO-coated quartz substrate, an emission layer of PDPSiEt, and an indium-containing magnesium (In : Mg) electrode. The spin-coated polymer film thickness ranged from 60 to 300 nm, depending on the concentration of PDPSiEt in the chloroform solution. The sample thickness was measured by a surfometric technique. The conditions of spin coating were 250 rpm for the first 5 s and then 2000 rpm for 30 s. The electrode area was 2 mm^2. A mixture of magnesium and indium was deposited on a spin-coated PDPSiEt film in a high vacuum below 10^{-4} Pa.

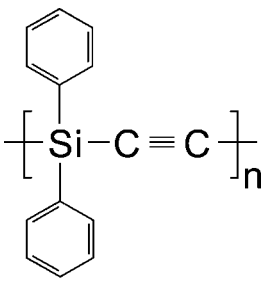

Scheme 1 Chemical structure of PDPSiEt.

Optical absorption and PL spectra were measured with a Hitachi (Tokyo, Japan) 330 spectrophotometer and a Hitachi F-2000 fluorescence spectrophotometer, respectively. The EL emission intensity was measured with a photomultiplier (R 928, Hamamatsu Photonics Co.). Current–voltage characteristics were measured with a conventional method with a Keithley (Cleveland, OH) 6517A electrometer, and the emission spectra were observed with a system combining a monochromator, photomultiplier, and lock-in amplifier (the EL diodes were operated in the pulse current mode). All measurements of the electric characteristics were performed in a cryostat at the temperature of liquid nitrogen (77 K). The ionization potential was measured by the ultraviolet photoelectron spectroscopy (UPS) method with a VG ESCA 3 Mk II (Beverly, MA) electron spectrometer.

QUANTUM CHEMICAL MODELING

Quantum chemical calculations were performed with *ab initio* and semiempirical quantum chemical methods (Gaussian computer program[17]). Isolated oligomers were taken into account, and their conformations were assumed to have central symmetries.

The conformations were determined by means of the minimization of the total energy calculated with the Becke three-parameter hybrid method with the correlation functional of Lee, Yang, and Paar (B3LYP). This method is known to give good conformational geometries and infrared (IR) spectra. The ultraviolet–visible spectrum was calculated by the semiempirical ZINDO method.

RESULTS AND DISCUSSION

The shape of the molecule, obtained by B3LYP quantum chemical *ab initio* calculations with the 3-21G(*) basis set of atomic orbitals, is given in Figure 1. The —C≡C—H units are taken as the ends of the molecule; thus, hexamer skeleton H—C≡C—[Si—C≡C]$_6$—H has been used for the calculations. The C—Si—C angles are about 108° through the entire oligomer structure. A similar result has been obtained by the Hartree–Fock method. The angle of C[Ph(4a)]—Si(4)—C[Ph(4b)] (for the numbering, see Fig. 1) has been determined to be 111°, the Si—C bond lengths through the entire oligomer skeleton are about 1.82 Å, and the C≡C bond length is around 1.22 Å. The calculation of the charge distribu-

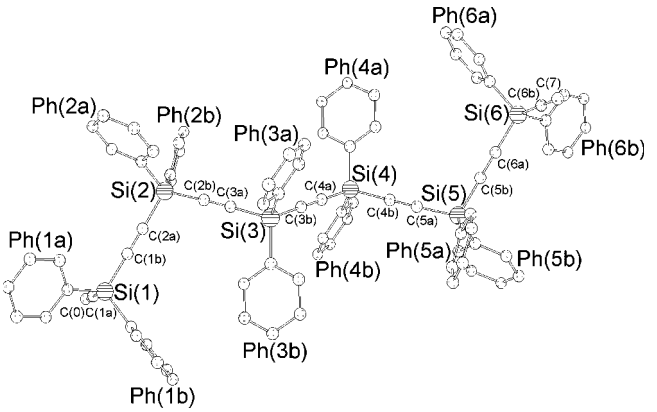

Figure 1 Geometry of oligo[(diphenylsilanediyl)ethynediyl] obtained by the B3LYP/3-21G(*) quantum chemical method. The numbering of the atoms is given.

tion (Mulliken charges) has given the following results: the silicon atoms are positively charged, bearing a unit charge of about 0.35, whereas the carbon atoms on the backbone are negatively charged with an average unit charge of −0.09. The rest of the negative charge is located on phenyls, with a unit charge of about −0.08 to −0.09 per phenyl.

The experimental IR spectrum of a thin film deposited from a solution onto a KBr disc, together with the theoretical B3LYP-calculated spectrum for the dimer, is given in Figure 2. The characteristic frequencies are summarized in Table I. The results of the calculations, made by means of the less cpu-time-consuming Hartree–Fock method, show that the extension of the oligomer length from the dimer to the tetramer does not substantially change the character of the spectrum. For this reason, we believe it is reasonable to compare the calculated dimer spectrum with the experimental polymer spectrum. We can see quite good agreement for the theoretical and experimental spectra, especially for peaks at frequencies of 475, 500, 697, 739, 789, 1115, 1185, and 1428 cm^{-1}. The experimental peaks at 3018, 3065, and 3426 cm^{-1} can be found in the theoretical spectrum, but they are a little frequency-shifted. The theoretical peaks located at 630 and 641 cm^{-1} can be ascribed to Si—C vibrations of the end groups; therefore, they cannot be found in the experimental spectrum. Similarly, the peak at 2103 cm^{-1} in the theoretical spectrum can be ascribed to the C≡C stretching of the end groups.

The absorption spectrum of PDPSiEt is given in Figure 3. It consists of a strong peak at about 200 nm, shoulders at 210 and 230 nm, and a very weak absorption in the region around 270 nm. As obtained by the ZINDO calculations, the main electronic transitions are related to π(phenyl and C≡C) → σ(main chain) and π(phenyl) (λ = 218 nm), π(phenyl and C≡C) → π(phenyl) (λ = 213 nm), π(phenyl) → π(phenyl) (λ = 211 nm), π(C≡C) → σ(main chain) (λ = 202 and 205 nm), and π(C≡C) → σ(main chain) and π(phenyl) (λ = 194–197 nm).

From an analysis of the experimental absorption edge under the assumption of direct electronic transitions with the relationship $(h\nu \times \alpha)^2$ versus $h\nu$, where $h\nu$ is the photon energy and α is the absorption coefficient, the band-gap energy has been evaluated to be 5.2 eV. By the calculation, the highest occupied molecular orbital (HOMO)/lowest unoccupied molecular orbital (LUMO) energy gap has been determined to be 5.33 eV, which is in good agreement with the experimental value.

Figure 4 shows PL and EL emission spectra of PDPSiEt films 180 nm thick. The EL spectrum is nearly independent of the applied voltage and also of the PDPSiEt film thickness. The PL spectrum is a good mirror image of the absorption spectrum, keeping even the shoulder. The Stokes shift of the fluorescence spectrum from the absorption spectrum is about 154 nm in the solid state. The peak in the EL spectrum (λ = 361 nm) almost coincides with that in the PL spectrum (λ = 354 nm), including a tail up to 570 nm. The external quantum emission efficiency at the maximum of the EL, calculated in terms of emitted photons per transported electrical charge, is 0.01%, that is, 9 cd/m^2 at the current density of 0.013 A/cm^2. Although the reported luminance is at least 1 order of magnitude lower than any industrial requirements, the result is interesting because not so many polymers show the ability to emit UV light. No geometrical or film-thickness optimization has been carried out. The main peak of the EL spectrum is narrower than that of the PL spectrum (the values of the full width at half-maximum are 0.48 and 0.69 eV).

The current–voltage curve of the ITO/PDPSiEt/In : Mg EL diode is given in Figure 5(a). The forward

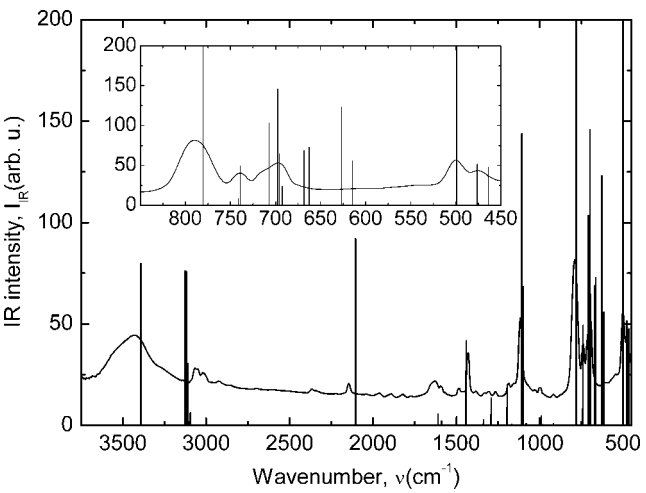

Figure 2 Experimental IR spectrum of PDPSiEt together with the theoretical spectrum obtained by the B3LYP/6-31G* method. The inset shows the region of 450–850 cm^{-1} in detail.

TABLE I
Characteristic IR Frequencies of Di[(diphenylsilanediyl)ethynediyl] Obtained by the Ab Initio B3LYP/6–31G* Method

No.	Experimental frequency (cm^{-1})	Calculation		Assignment
		Frequency (cm^{-1})	IR intensity (km/mol)	
1	—	308.1	19.5	Main-chain vibrations
2	—	395.8	33.9	Phenyl deformation (twist)
3	—	400.5	67.1	
4	475.5	464.0	47.7	Out-of-plane ring deformation
5		476.2	51.6	
6	500.3	499.1	246.6	C≡C—Si bending
7	—	614.5	55.9	In-plane ring deformation mixed
8	—	626.7	123.1	with main-chain vibrations
9	—	662.7	73.0	C—H bending at the chain end
10	—	668.3	68.9	
11	697.1	692.7	23.9	Out-of-plane phenyl C—H bending
12		695.8	64.8	
13		697.4	145.9	
14		707.3	103.6	Phenyl and chain-end C—H bending
15	739.3	739.1	49.4	Out-of-plane phenyl C—H bending
16	789.6	780.3	638.4	Main-chain Si—C stretching
17	1114.9	1100.4	68.5	Si—phenyl stretching
18		1106.8	143.9	
19	1185.2	1194.3	20.2	In-plane phenyl C—H bending
20	1265.0	1289.3	13.6	Phenyl C—C stretching
21	1428.0	1438.7	41.8	In-plane phenyl C—H bending
22		1440.9	27.0	
23	2144.3	2103.4	92.1	C≡C stretching at the chain end
24	3019.0	3109.7	30.7	Phenyl C—H stretching
25		3110.0	10.4	
26		3117.7	64.5	
27		3117.9	75.8	
28		3125.9	76.2	Phenyl C—H stretching (symmetrical)
29		3126.3	45.8	
30	3426.4	3392.0	79.8	C—H stretching at the chain end

A uniform frequency scaling factor of 0.975 was used.

bias corresponds to a positive bias voltage on the ITO electrode. The current increases with increasing voltage, but the reverse bias current remains small; the diode exhibits a typical rectifying characteristic. The light emission starts at about 8 V in a sample with a thickness of 180 nm. The dependence of the integral emission intensity on the injection current is given in Figure 5(b). The emission intensity increases monotonically with increasing injection current, showing

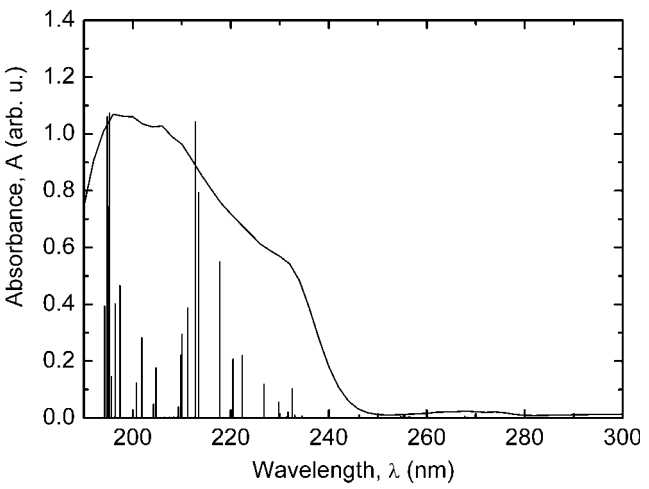

Figure 3 Absorption spectrum of a thin PDPSiEt film. The discrete lines are the calculated electronic transitions; their heights represent the relative values of the oscillator strength.

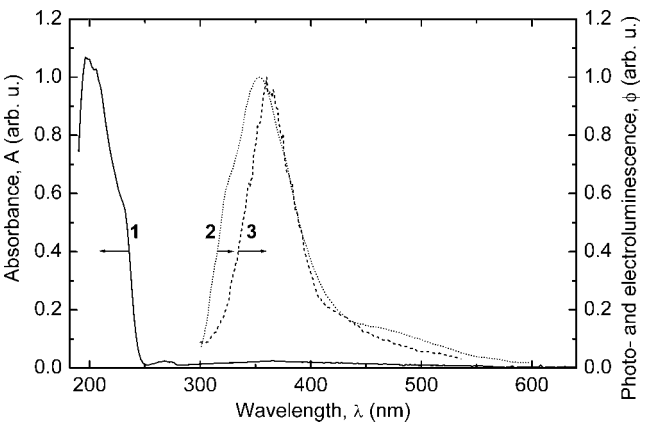

Figure 4 (1) Absorbance, (2) PL, and (3) EL spectra of thin PDPSiEt films. The applied voltage was 10 V, and the film thickness was 180 nm.

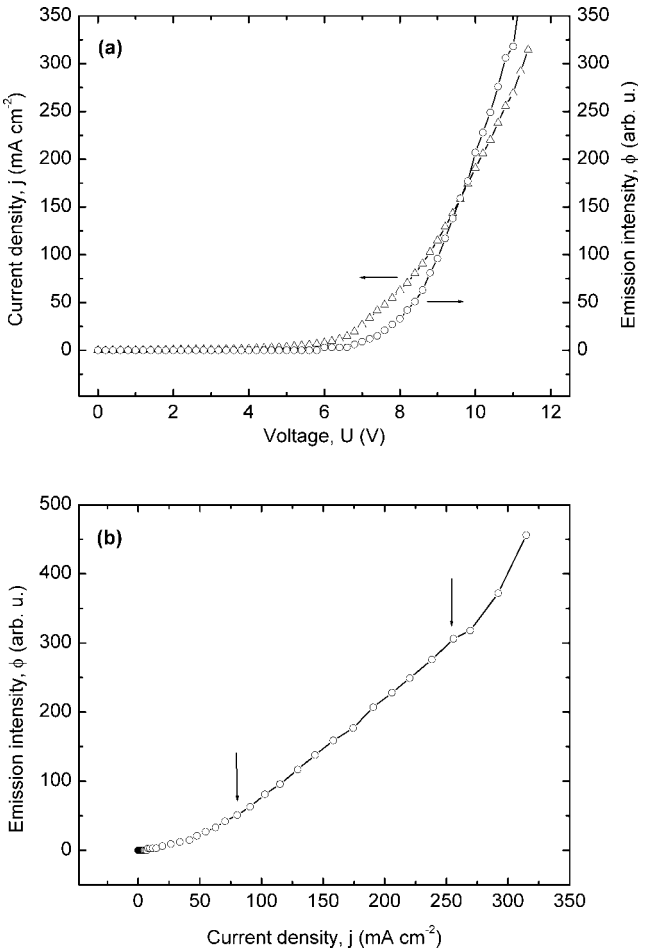

Figure 5 (a) Current–voltage and intensity–voltage and (b) intensity–current curves for thin PDPSiEt films measured at 77 K. The film thickness was 180 nm.

almost a linear dependence in the voltage range of 3–11 V (cf. the arrows).

Figure 6 shows band diagrams of the ITO/PDPSiEt/In diode without and with an applied voltage. The work function of the cathode (indium) defines the offset between the Fermi energy of the cathode and the LUMO level in PDPSiEt at about 1.8 eV. The barrier between the Fermi level in In and the LUMO level of PDPSiEt (2.4 eV) is quite high, and the number of injected electrons is reduced. A similar barrier (2.3 eV) is formed between the ITO electrode and PDPSiEt. Thus, we can expect that for low applied voltages, the hole injection will also be reduced and the current will be limited by a precontact barrier. The position of the HOMO level has been determined by the electron spectroscopy for chemical analysis method in a solid film as the first ionization potential. Because PDPSiEt is a hole-transporting polymer, the charge recombination and exciton formation take place mostly at the cathode, whereas the anode is mainly responsible for the injection of movable charges.

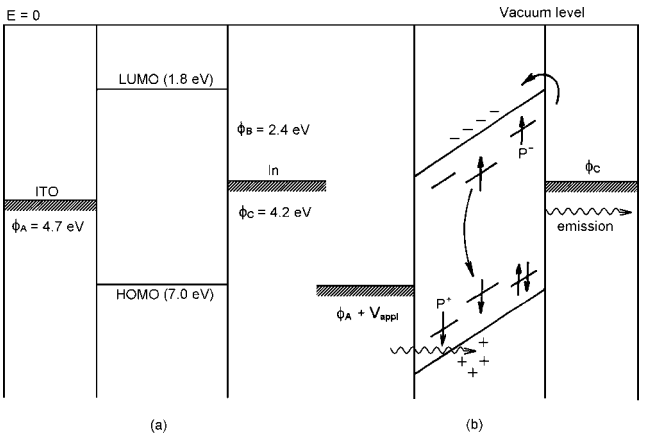

Figure 6 Band diagrams of the ITO/PDPSiEt/In diode (a) without and (b) with an applied voltage (V_{appl}). ϕ_A and ϕ_C are the work functions of ITO and indium, respectively. ϕ_B is the barrier between the Fermi level in In and the LUMO level of PDPSiEt. P^+ and P^- are the levels of positive and negative polarons, respectively.

The current–voltage curve of the ITO/PDPSiEt/In diode is highly nonlinear, as shown in Figure 5. There are three basic charge-generation mechanisms that can be invoked to explain the shape of the current–voltage curve. The first concerns space-charge-limited injection,[18–21] the second concerns Richardson–Schottky thermionic emissions, and the third concerns Fowler–Nordheim tunnelling.[22]

The current density versus the voltage in double-logarithmic coordinates is given in Figure 7. The first region up to voltage U_1 is typical for Fowler–Nordheim tunneling. The theory predicts[22] the electrical field dependence of the current density in the following form:

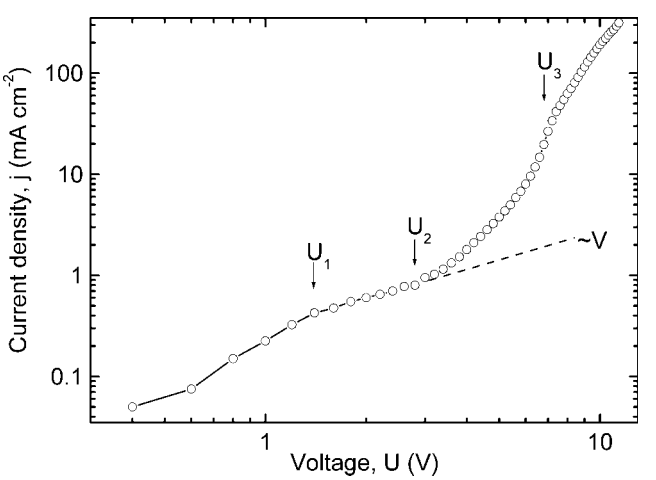

Figure 7 Current–voltage curve for a thin PDPSiEt film measured at 77 K in double-logarithmic coordinates. The film thickness was 180 nm.

$$j \sim F^2 \exp\left(-\frac{K}{F}\right) \quad (1)$$

where j is the current density, K is a parameter that depends on the barrier shape, and F is the electric field strength.

The linear part of the curve of the current density versus the voltage in the region of $U_1 = 1.5$ V to $U_2 = 3$ V suggests a contact-limited-current, superlinear behavior in the U_2–U_3 voltage region results from the lowering of the barrier. At higher voltages, the current is influenced by double injection. No experimental evidence for pure space-charge injection has been observed. Thus, the charge tunneling through a precontact barrier can be assumed. The reproducibility of the current–voltage curves for various samples is ordinary for this type of measurement.

The charge-carrier emission from the ITO electrode leads to the formation of a positive polaron. After the polaron formation, the shape of the molecule is changed. Figure 8 shows the geometry of the positive and negative polarons, as obtained by calculations with the B3LYP/3-21G(*) method. Figure 9 demonstrates the changes in the bond lengths and C—Si—C angles of the molecule during the polaron formation. Although during the positive polaron formation the bond lengths (both Si—C and C≡C) do not change much in comparison with the neutral molecule, during the formation of the negative polaron, the C≡C bond is lengthened by about 5%, whereas some Si—C bonds become shorter. The C—Si—C angles becomes smaller in the positive polaron formation and larger during the formation of the negative polaron. During the formation of the positive polaron, Si atoms become more positive, whereas C atoms in the main chain carry approximately the same charge as the neutral molecule. During the formation of the negative polaron, all atoms in the backbone are more negative. Charges on phenyls are more positive or negative in the formation of the positive or negative polaron, respectively.

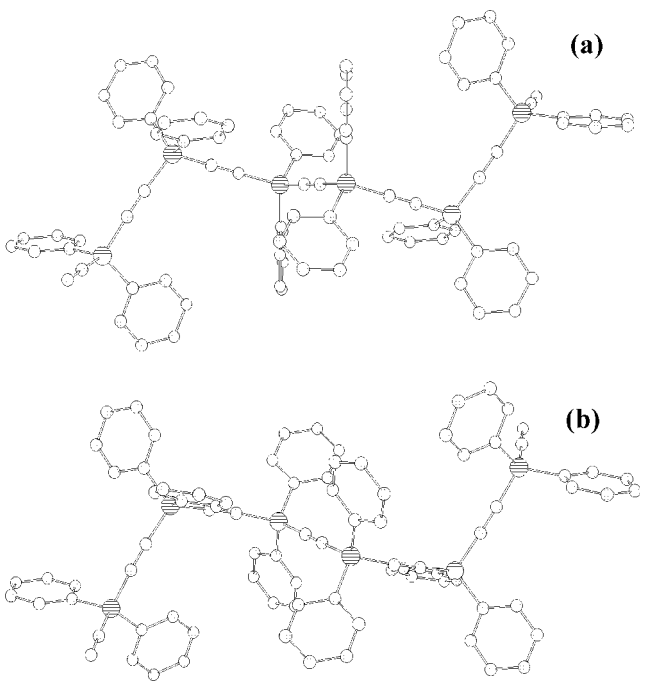

Figure 8 Geometry of (a) positively and (b) negatively charged oligo[(diphenylsilanediyl)ethynediyl] obtained by the quantum chemical B3LYP/3-21G(*) method.

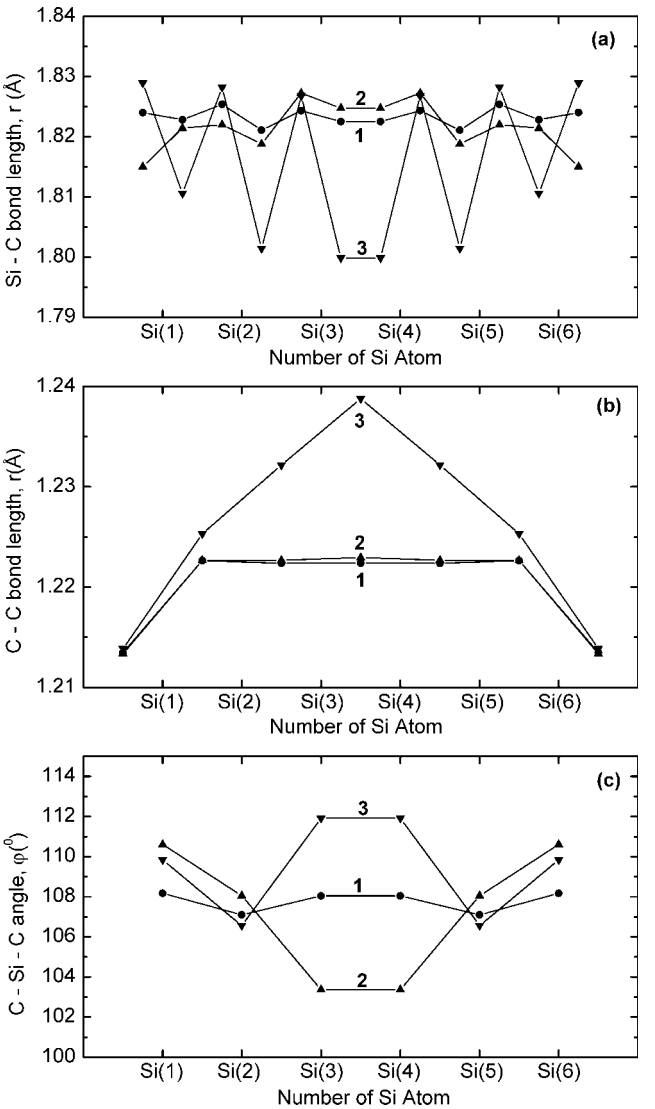

Figure 9 (a) Si—C and (b) C≡C bond length distributions and (c) C—Si—C angle distributions through the oligomer chain obtained by the B3LYP/3-21G(*) method for (1) neutral PDPSiEt, (2) a positive polaron, and (3) a negative polaron.

CONCLUSIONS

A new polymeric wide-band-gap semiconductor has been prepared, and its optical and EL properties have been studied. The band-gap energy has been deter-

mined to be 5.2 eV, and the PL maximum has been observed at $\lambda = 354$ nm. The material is suitable for the fabrication of UV EL diodes. The EL spectrum of the ITO/PDPSiEt/In : Mg diode consists of a strong peak at 361 nm and a tail up to 570 nm. The spectrum is nearly independent of the applied voltage and the film thickness. The peak in the EL spectrum (maximum wavelength = 361 nm) almost coincides with that in the PL spectrum. The intensity of the emitted light at the EL maximum is 9 cd/m^2 at a current density of 0.013 A/cm^2 (no geometrical or thickness optimization has been carried out). The absorption spectrum is a good mirror image of the luminescence spectrum. The electric characteristics are influenced by tunneling through an interface barrier at the contact.

The computer time at the MetaCenter (Prague and Brno) and the Joint Supercomputing Center at Czech Technical University is gratefully acknowledged. The authors are grateful to J. Zemek for the electron spectroscopy for chemical analysis measurements.

References

1. Helfrich, W.; Schneider, W. G. Phys Rev Lett 1965, 14, 229.
2. Pope, M.; Swenberg, C. E. Electronic Processes in Organic Crystals; Oxford University Press: New York, 1999; see also the references therein.
3. Tang, C. W.; VanSlyke, S. A. Appl Phys Lett 1987, 51, 913.
4. Tang, C. W.; VanSlyke, S. A.; Chen, C. H. J Appl Phys 1989, 65, 3610.
5. Burroughes, J. H.; Bradley, D. D. C.; Brown, A. R.; Marks, R. N.; MacKay, K.; Friend, R. H.; Burn, P. L.; Holmes, A. B. Nature (London) 1990, 347, 539.
6. Photonic and Optoelectronic Polymers; Jenekhe, S. A.; Wynne, K. J., Eds.; American Chemical Society: Washington, DC, 1997.
7. Greenham, N. C.; Moratti, S. C.; Bradley, D. D. C.; Friend, R. H.; Holmes, A. B. Nature (London) 1993, 365, 628.
8. Fujii, A.; Yoshimoto, K.; Yoshida, M.; Ohmori, Y.; Yoshino, K. J Soc Electr Mater Eng 1995, 4, 59.
9. Fujii, A.; Yoshimoto, K.; Yoshida, M.; Ohmori, Y.; Yoshino, K.; Ueno, H.; Kakimoto, M.; Kajima, H. Jpn J Appl Phys 1996, 35, 3914.
10. Abkowitz, M. A.; Stolka, M. J Non-Cryst Solids 1989, 114, 342.
11. Nešpůrek, S.; Valerián, H.; Eckhardt, A.; Herden, V.; Schnabel, W. Polym Adv Technol 2001, 12, 306.
12. Suzuki, H.; Meyer, H.; Simmerer, J.; Yang, J.; Haarer, D. Adv Mater 1993, 5, 743.
13. Organic Electroluminescent Materials and Devices; Miyata, S.; Nalwa, H. S., Eds.; Gordon & Breach: Amsterdam, 1997.
14. Qiu, C. F.; Wang, L. D.; Chen, H. Y.; Wong, M.; Kwok, H. S. Appl Phys Lett 2001, 79, 2276.
15. Yoshino, K.; Tada, K.; Hirohata, M.; Hidoyat, R.; Tatsuhara, S.; Ozaki, M.; Naka, A.; Ishikawa, M. Jpn J Appl Phys 1997, 36, L1548.
16. Fang, M.-C.; Watanabe, A.; Matsuda, M. Chem Lett 1994, 1, 13.
17. Frisch, M. J.; Trucks, G. W.; Schlegel, H. B.; Scuseria, G. E.; Robb, M. A.; Cheeseman, J. R.; Zakrzewski, V. G.; Montgomery, J. A.; Stratmann, R. E.; Burant, J. C.; Dapprich, S.; Millam, J. M.; Daniels, A. D.; Kudin, K. N.; Strain, M. C.; Farkas, O.; Tomasi, J.; Barone, V.; Cossi, M.; Cammi, R.; Mennucci, B.; Pomelli, C.; Adamo, C.; Clifford, S.; Ochterski, J.; Petersson, G. A.; Ayala, P. Y.; Cui, Q.; Morokuma, K.; Malick, D. K.; Rabuck, A. D.; Raghavachari, K.; Foresman, J. B.; Cioslowski, J.; Ortiz, J. V.; Stefanov, B. B.; Liu, G.; Liashenko, A.; Piskorz, P.; Komaromi, I.; Gomperts, R.; Martin, R. L.; Fox, D. J.; Keith, T.; Al-Laham, M. A.; Peng, C. Y.; Nanayakkara, A.; Gonzalez, C.; Challacombe, M.; Gill, P. M. W.; Johnson, B.; Chen, W.; Wong, M. W.; Andres, J. L.; Gonzales, C.; Head-Gordon, M.; Replogle, E. S.; Pople, J. A. Gaussian 98, Revision A.7; Gaussian: Pittsburgh, PA, 1998.
18. Nešpůrek, S.; Sworakowski, J. J Appl Phys 1980, 51, 2098.
19. Zmeškal, O.; Schauer, F.; Nešpůrek, S. J Phys C: Solid State Phys 1985, 18, 1873.
20. Sworakowski, J.; Nešpůrek, S. J Appl Phys 1989, 65, 1559.
21. Nešpůrek, S.; Sworakowski, J. Radiat Phys Chem 1990, 36, 3.
22. Fowler, R. H.; Nordheim, L. Proc R Soc London Ser A 1928, 119, 173.